Supplementary Information

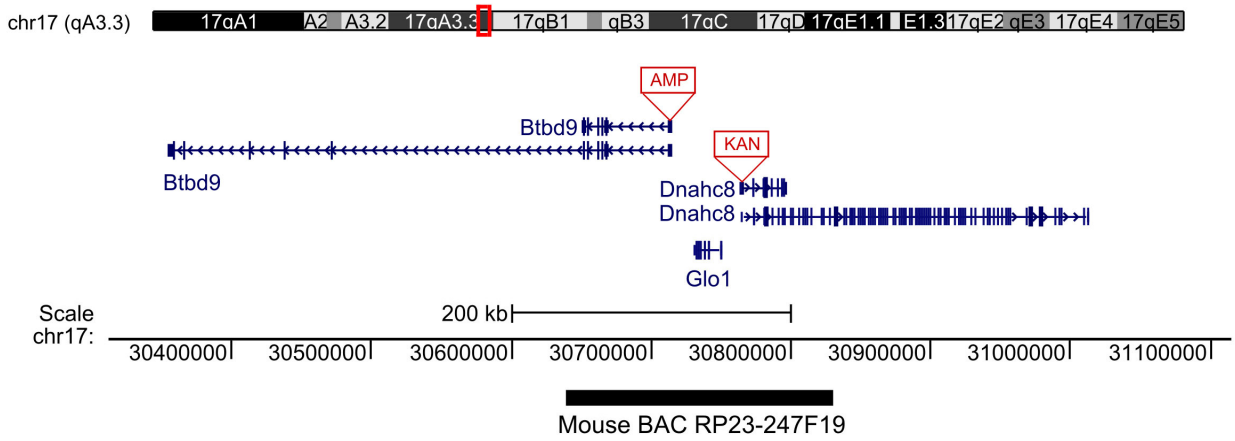

Figure S1: Schematic of the recombineered BAC

The mouse BAC RP23-247F19 was modified using RED/ET recombination. The BAC contains *Glo1* and partial copies of *Btbd9* and *Dnahc8*. To prevent expression of alternatively spliced variants of *Btbd9* and *Dnach8*, ampicillin (AMP) and kanamycin (KAN) cassettes were inserted into the BAC to replace the first exons of these genes, respectively.

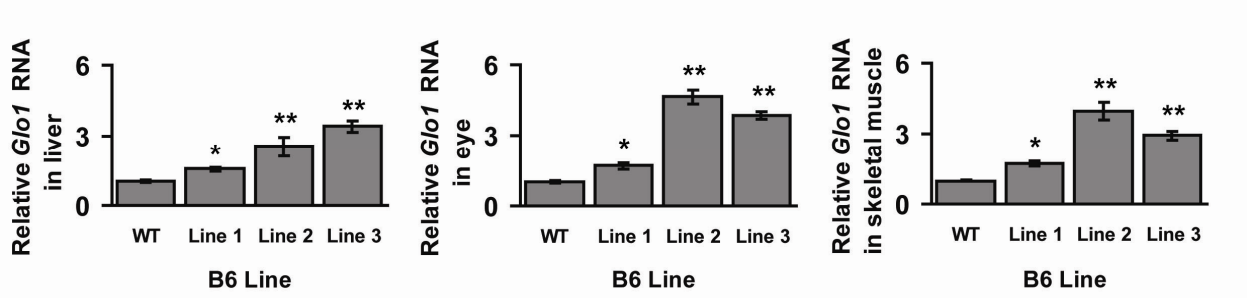

Figure S2: *Glo1* mRNA expression in peripheral tissues

Glo1 mRNA was measured in liver (left), eye (middle), and skeletal muscle (right) of WT and Tg mice from each B6 line. These tissues were selected, because they have high levels of *Glo1* mRNA expression. One-way ANOVAs: $P < 10^{-9}$ (liver), $P < 10^{-15}$ (eye), $P < 10^{-10}$ (skeletal muscle).

Data are mean ± SEM. BAC, Bacterial Artificial Chromosome; WT, wild type; Tg, transgenic.*$P < 0.0075$, **$P < 0.0001$; n=10–12 WT, 3–7 Tg per line.

	Line	BAC Copy Number	Proportion of Tg Offspring	Tg Proportion higher or lower vs. expected	Body Position	Righting reflex	Toe pinch reflex	Ear twitch reflex	Whisker placing response	Whisker orienting reflex	Eye blink reflex	Visual placing response†	Balance beam
B6	WT	0			6	6/6	6/6	6/6	6/6	6/6	6/6	6/6	0.333
	Line 1	2	0.398*	Lower	6	3/3	3/3	3/3	3/3	3/3	3/3	3/3	0.333
	Line 2	8	0.458	-	6	3/3	2/3	3/3	3/3	3/3	3/3	3/3	0.333
	Line 3	10	0.363*	Lower	6	4/4	4/4	4/4	4/4	4/4	4/4	4/4	0.25
FVB	WT	0			6	6/6	6/6	6/6	6/6	6/6	6/6		0.333
	Line 1	2	0.418*	Lower									
	Line 2	7	0.500	-	6	4/4	4/4	4/4	4/4	4/4	4/4		0.5
	Line 3	28	0.636*	Higher	6	1/1	1/1	1/1	1/1	1/1	1/1		0
	Line 4	35	0.356*	Lower	6	2/2	2/2	2/2	2/2	2/2	2/2		0
	Line 5	50	0.478	-	6	2/2	2/2	2/2	2/2	2/2	2/2		0

Table S1: Reproduction rate, general health, and reflexes of Tg mice

The proportion of Tg mice produced from each line was measured. The expected proportion was 0.5; deviation from the expected rate was assessed by a Chi-square test. Tg proportions that significantly differed from expected are indicated by an asterisk (*). All together, 4 lines had lower, 1 line had higher, and 3 lines had the expected Tg proportion. Tg proportion was not at all correlated with BAC copy number. Therefore, we conclude that the BAC does not decrease fitness. Decreased Tg proportion in some lines is more likely due to integration effects rather than an effect of *Glo1* overexpression.

Tg mice appeared normal, and were not visually discernible from their WT littermates. WT and Tg mice from B6 and FVB lines were tested for body position, neurological reflexes, vision, and motor coordination. Body position was scored on a scale of 1-8 (1) and is

Table S1 (continued)

reported as the mean. The presence (1) or absence (0) of reflexes was measured; data are reported as the fraction of mice with the reflex present. The balance beam test was used to assess motor coordination; data are reported as mean footslips. WT and Tg mice did not significantly differ in any of these parameters, indicating that Tg mice do not have deficits that could interfere with the interpretation of behavioral tests of anxiety.

† The visual placing reflex was not measured in FVB mice, because they are homozygous for the *Pde6b*^{rd1} allele, which results in early onset retinal degeneration (http://jaxmice.jax.org/strain/001800.html). WT, wild type; Tg, transgenic.

Probe set ID	Gene symbol	mRNA accession	Genomic location	Fold change (Tg v. WT)	q-value	Validated by qPCR in Tg Line 3?	Validated by qPCR in all Tg lines?
10536444	*Foxp2*	NM_053242	chr6:15135506-15391977	0.64	0.0029*	Yes	No
10449644	*Glo1*	NM_025374	chr17:30729807-30749604	2.81	0.0029*	Yes	Yes
10543145	*Thsd7a*	NM_001164805	chr6:12261608-12699253	0.63	0.0029*	Yes	No
10471675	*Glo1*	NM_025374	chr17:30729807-30749604	2.85	0.0099*	Yes	Yes
10536407	*Phf14*	NM_029404	chr6:11875881-12031198	0.53	0.022*	Yes	No
10543134	*Ndufa4*	NM_010886	chr6:11850373-11857446	0.58	0.027*	Yes	No
10449631	*Btbd9*	NM_027060	chr17:30352469-30713232	1.19	0.99		
10443598	*Dnahc8*	NM_013811	chr17:30940008-30950175	1.11	0.99		
10449652	*Dnahc8*	NM_013811	chr17:30940008-30950175	0.99	--		

Table S2: Microarray analysis of whole-brain mRNA from WT and Tg mice

Whole-brain mRNA was purified from WT and Tg littermates from B6 Line 3. *P*-values were converted to q-values, and q-values < 0.05 were considered statistically significant (indicated by an asterisk). Only genes that were significantly differentially expressed between WT and Tg were measured by qPCR. All differentially expressed genes identified by the microarray were validated by qPCR in Tg Line 3. However, when the expression of these genes was measured by qPCR in Tg Lines 1 and 2, only *Glo1* was differentially expressed. Importantly, the other 4 genes identified by the microarray were located on the same region of chromosome 6. Therefore, the transgene likely inserted into this region, disrupting the expression of neighboring genes. Because each Tg line has a different transgenic insertion site, these genes were not disrupted in the other lines. Importantly, the other 2 genes in the BAC (*Btbd9* and *Dnahc8*) were not differentially expressed between WT and Tg. Therefore, with the sample size used, no genes were significantly differentially expressed between WT and Tg mice.

Table S2 (continued)

Complete microarray data are available from GEO (accession number GSE36819). qPCR data for *Glo1* are presented in Figure 1C in the main text. qPCR data for *Foxp2*, *Thsd7a*, *Phf14*, and *Ndufa4* are not shown. n = 5 WT, 5 Tg from B6 Line 3. qPCR, quantitative real-time PCR; WT, wild type; Tg, transgenic.

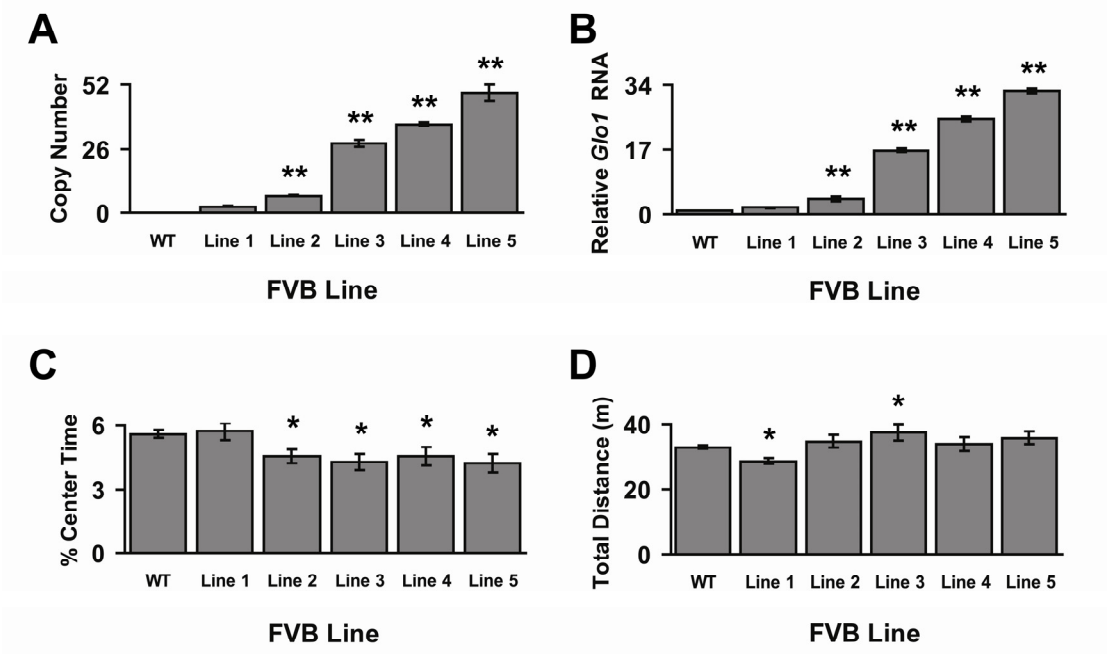

Figure S3: BAC copy number, *Glo1* expression, and anxiety-like behavior in FVB Tg lines

5 lines of Tg mice were generated on an FVB/NJ (FVB) background using the same BAC construct used for generating B6 Tg mice (Figure 1A and S1A). WT mice from each line were pooled into a common WT group. **A,** BAC copy number was measured in each FVB line by qPCR on genomic DNA. One-way ANOVA, $P < 10^{-9}$; n = 33 WT, 4–14 Tg per line. **B,** *Glo1* mRNA was measured in whole brain of WT and Tg mice from each FVB line using qPCR. One-way ANOVA, $P < 10^{-15}$; n = 17 WT, 3–7 Tg per line. **C,** Center time in the OF test: WT and Tg littermates from each FVB line were tested in the OF test. One-way ANOVA, $P = 0.0015$; n = 111 WT, 14–22 Tg per line. **D,** A one-way ANOVA was significant for the effect of genotype ($P = 0.003$) on locomotor activity. While decreased locomotor activity can confound the interpretation of decreased center time in the OF test (2), only one FVB Tg mice displayed decreased total distance (Tg Line 1). Another displayed increased total distance (Tg Line 3), and the remainder did not significantly differ from WT. Therefore, decreased center time is not confounded by decreased locomotor activity.

Figure S3 (continued)

Data are mean ± SEM. *$P < 0.05$, **$P < 0.0001$. BAC, bacterial artificial chromosome; OF, open field; qPCR, quantitative real-time PCR; WT, wild type; Tg, transgenic.

Genotype	*n*	% Time in Light	*P*-value
B6 WT	10	40.5 ± 3.3	0.028
B6 Tg	12	31.6 ± 2.1	
FVB WT	11	37.5 ± 4.3	0.041
FVB Tg	10	26 ± 2.8	

Table S3: *Glo1* overexpression increases anxiety-like behavior in the light-dark box test

WT and Tg littermates from the B6 and FVB lines with the highest copy number (B6 Line 3 and FVB Line 5, respectively) were tested in the LD box test. Tg mice spent significantly less time in the light compartment compared to their respective WT controls, indicating increased anxiety-like behavior. WT and Tg mice did not differ in transitions between the compartments (data not shown).

Data are mean ± SEM. WT, wild type; Tg, transgenic; LD, light-dark.

Genotype	*n*	% Open Arm Entries	*P*-value	Total Entries	*P*-value
FVB WT	8	35.2 ± 3.7	0.044	19.6 ± 1.5	0.20
FVB Tg	10	22.8 ± 4.1		15.9 ± 2.2	

Table S4: *Glo1* overexpression increases anxiety-like behavior in the elevated plus maze

WT and Tg littermates from FVB Line 4 were tested in the EPM. Tg mice made significantly fewer entries into the open arms compared to WT mice, indicating increased anxiety-like behavior. WT and Tg mice did not differ in total number of arm entries.

Data are mean ± SEM. WT, wild type; Tg, transgenic; EPM, elevated plus maze.

Treatment	MG concentration (nmol/g tissue)	Relative MG concentration (%)	Estimated MG concentration (μM)†
Vehicle	4.89 +/- 0.43	100.00	5.13
MG (50 mg/kg)	5.66 +/- 0.36	115.75	5.94
MG (100 mg/kg)	6.23 +/- 0.26	127.40	6.54
MG (300 mg/kg)	7.87 +/- 0.56	160.94	8.26

Table S5: Measurement of MG concentration in brain

WT B6 mice were treated i.p. with vehicle or MG (50, 100, or 300 mg/kg). MG concentration was then measured in the brain by HPLC as nmol/g tissue. Relative MG concentration was determined by normalizing values to those of vehicle-treated mice. †: MG concentration was converted to μM assuming a brain density of 1.05 g/mL.

The measured MG concentration was within the range of brain MG concentrations previously reported: 1.5 to 175 μM (3, 4). When we used the same MG detection method, we found MG concentration in the plasma to be 720 nM (± 150 nM, $n = 3$). Again, this is within the range of MG concentrations previously reported for blood, plasma, and serum: 50 nM – 4.5 μM (5-9). This demonstrates that the concentration of MG in the brain is higher than that in blood.

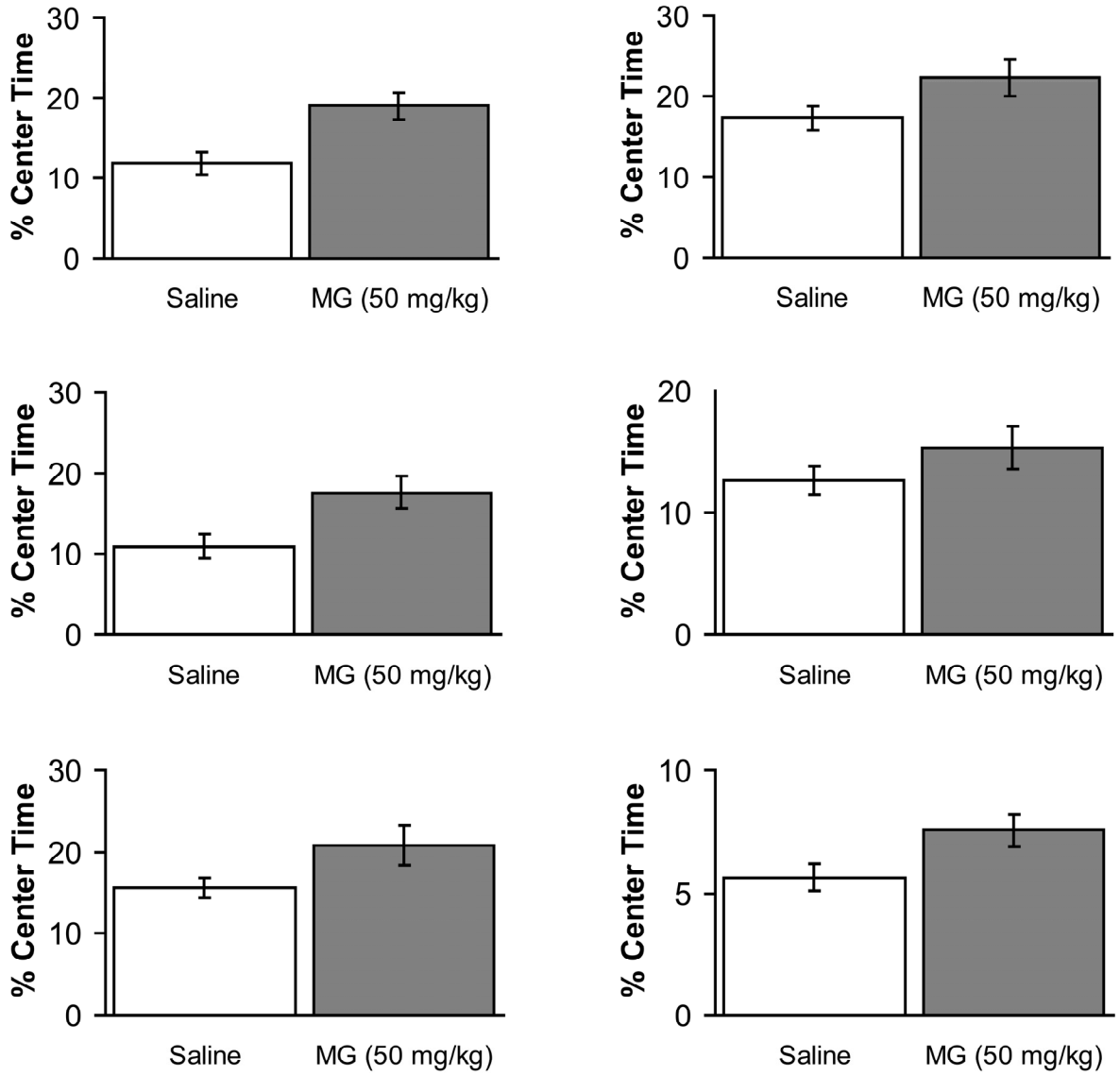

Figure S4: Replicate experiments demonstrating that acute MG treatment is anxiolytic in the open field test

Male B6 mice were treated i.p. with vehicle or MG (50 mg/kg). Ten or 20 minutes post-injection, mice were tested in the OF test for 5 or 10 minutes. Each panel represents an independent replication experiment. Data are mean ± SEM. Sample sizes ranged from 7–18 per group. MG, methylglyoxal; OF, open field.

Meta-analysis	
Cohen's *d*	0.7798
95% CI lower limit	0.4747
95% CI upper limit	1.0848
Meta-analysis *z*-score	5.0096
P-value	< 0.0001
Heterogeneity	
Q	4.0687
P-value	0.6674
H	1
95% CI lower limit	1
95% CI upper limit	1.8509
I^2	0%
95% CI lower limit	0%
95% CI upper limit	70.81%
t^2	0
Q-index	0%

Table S6: Meta-analysis of replication experiments demonstrating MG's anxiolytic effect in the open field test

A meta-analysis was used because of minor methodological differences between replication experiments (e.g., time post-injection, experimental apparatus). A meta-analysis was performed on a total of 7 individual experiments (the first demonstration plus 6 replication studies) using a fixed-effect model. Total $n = 181$. The meta-analysis revealed that MG had a large effect on anxiety-like behavior (Cohen's $d = 0.78$)(10). The result was statistically significant ($P < 0.0001$). Importantly, there was no significant heterogeneity among the studies, indicating that the outcomes were not due to random effects.

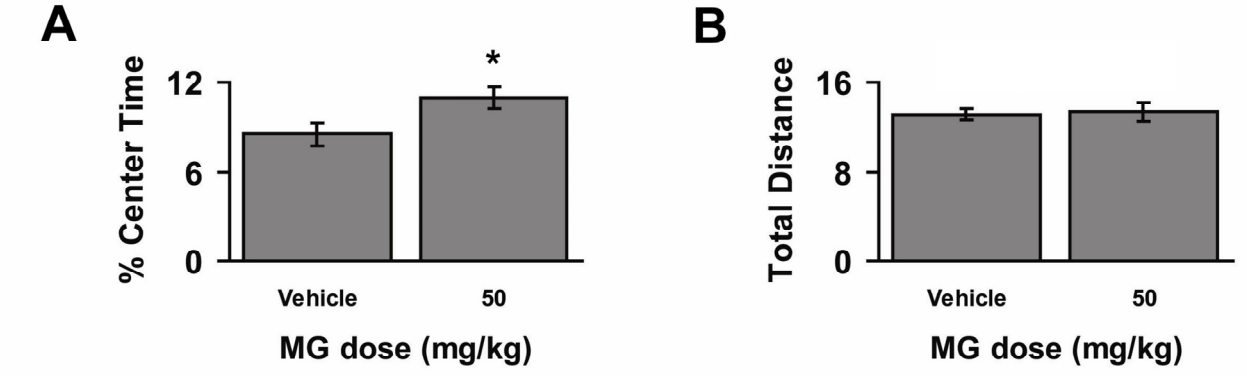

Figure S5: Acute MG treatment is anxiolytic in CD-1 mice

Male CD-1 mice were treated i.p. with vehicle or MG (50 mg/kg). Ten minutes post-injection, mice were tested in the OF test. $n = 27$ vehicle, 28 MG. **A**, MG treatment increased time in the center of the open field. **B**, MG treatment did not change total distance traveled.

MG, methylglyoxal; OF, open field. Data are mean ± SEM. *$P < 0.05$ by 2-tailed *t*-test.

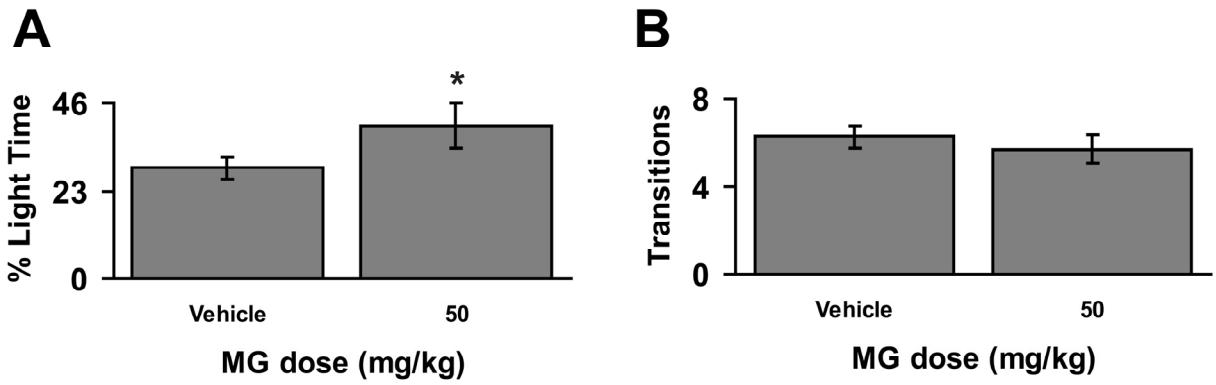

Figure S6: Acute MG treatment is anxiolytic in the light-dark box test

WT B6 mice were treated i.p. with vehicle or MG (50 mg/kg). Ten minutes post-injection, mice tested in the LD box test. **A**, Mice treated with MG spent significantly more time in the light compartment, indicating decreased anxiety-like behavior. **B**, MG treatment did not significantly change number of transitions between the compartments. This indicates that MG reduces anxiety-like behavior in the LD box test. $n = 16$ per group; * $P < 0.05$ by 1-tailed t-test.

WT, wild type; MG, methylglyoxal; LD, light-dark; OF, open field.

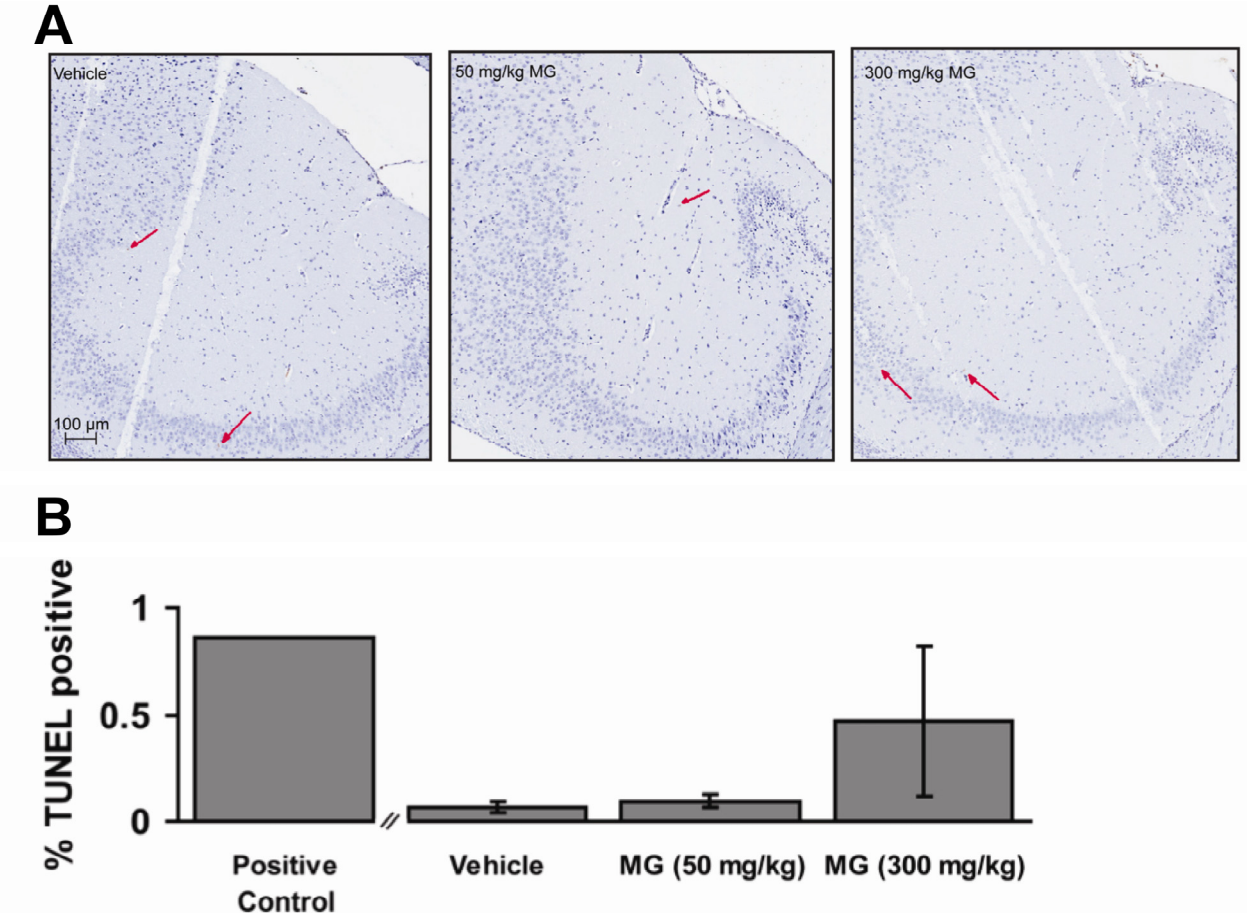

Figure S7: Quantification of apoptotic cells in the brain after MG administration

Male B6 mice were treated i.p. with vehicle or MG (50 or 300 mg/kg). Twenty-four hours after treatment, the brains were processed, and apoptotic cells were detected by *in situ* TUNEL staining. A positive control (female rodent mammary gland 3–5 days post-weaning) was stained and analyzed in parallel.

Neuropathological analysis of hematoxylin and eosin stained brain sections reveled no overt pathology in MG-treated mice (data not shown). There was a non-significant increase in positive TUNEL staining at the edges of the sections and immediately adjacent to blood vessels and ventricles in brain sections from MG-treated mice. This could be an artifact of tissue processing

Figure S7 (continued)

or could represent cells exposed to locally higher MG concentrations. **A**, There was no discernible difference in TUNEL staining in the brain tissue between vehicle- and MG-treated mice. Red arrows indicate TUNEL positive cells. **B**, Apoptotic cells were quantified in the hippocampus, a brain region particularly prone to neurotoxic insults (11). MG treatment did not significantly change levels of apoptosis in the hippocampus compared to vehicle treatment (one-way ANOVA for the factor treatment, $P > 0.3$). Although 300 mg/kg MG non-significantly increased apoptosis, this dose is near the LD_{50} for MG treatment (~ 400 mg/kg, determined experimentally). Importantly, 50 mg/kg MG did not significantly increase apoptosis, indicating that MG's anxiolytic effects are independent of its cytotoxic effects. Likewise, MG's time course for anxiolysis is different than that for cytotoxicity: MG is anxiolytic within minutes of administration, while it induces apoptosis hours after application (12).

MG, methylglyoxal. Data are mean ± s.e.m. $n = 4$ mice per group (3–4 sections per brain).

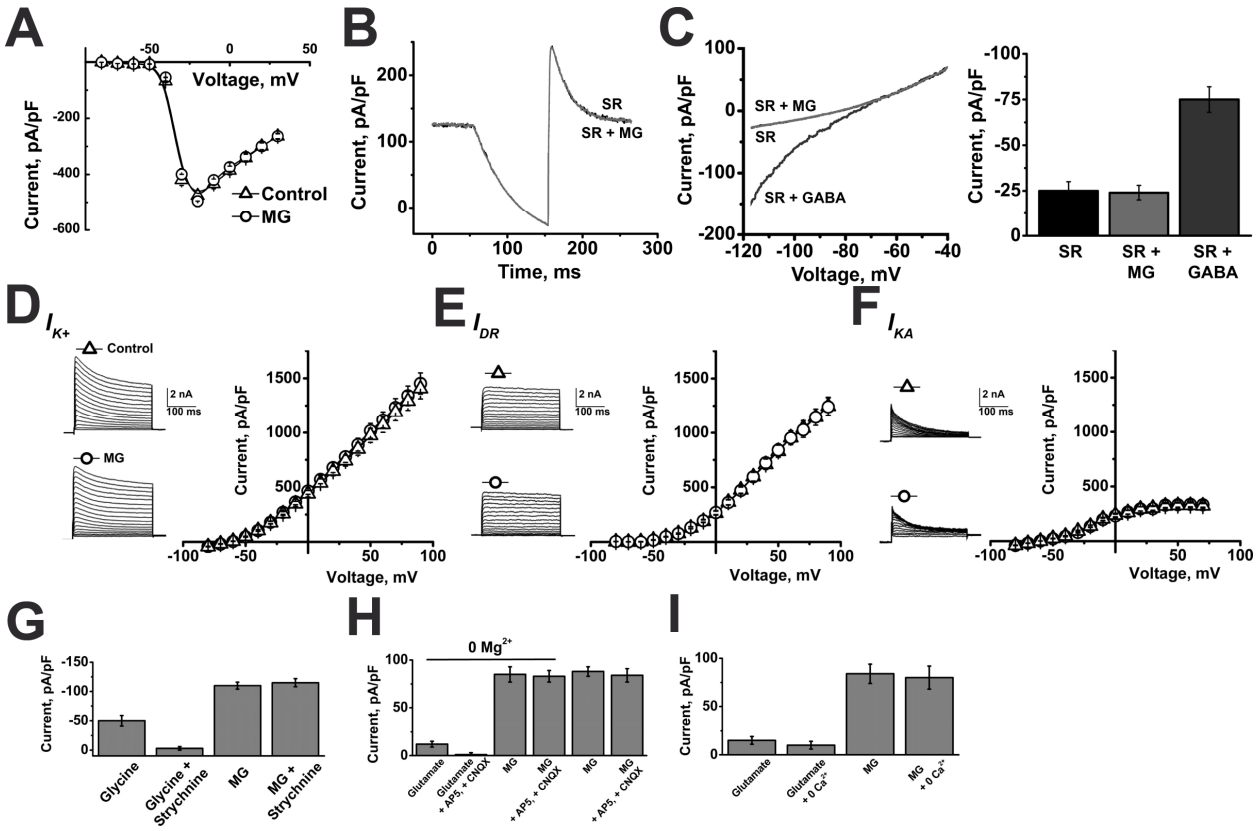

Figure S8: MG does not modulate other conductances in CGNs

A, I_{Na} Voltage-gated sodium currents were evoked by 100 ms step depolarizations between -80 and 30 mV. Mean current-density ± SEM is plotted against test voltage for ten cells studied during perfusion of the bath solution without (△) and then with 10 μM MG (O).

B, I_{Kso} The potassium leak current, I_{Kso}, was studied by voltage ramps from -20 mV to -120 mV at a rate of -1 mV/ms applied every 20 seconds. Currents were evoked in the presence of 10 μM SR-95531 (SR), to block $GABA_A$ receptors, and were not altered when 10 μM MG was added to the bath solution in the continued presence of SR (SR + MG).

C, I_{KIR} *Left*, Representative current-density ramps from the protocol described in B replotted against voltage. In the presence of SR or SR + MG, I_{Kso} showed open rectification and had a reversal potential close to E_{K+} (-80 mV), indicating potassium selectivity. In contrast, an inwardly rectifying, potassium-selective current was observed when 10 μM GABA was applied in the continued presence of SR (SR +

Figure S8 (continued)

GABA). In this case, GABA activates inwardly rectifying potassium currents via the interaction of $GABA_B$ receptors with K_{IR} channels. *Right*, a histogram of mean current-density ± SEM at -100 mV for 10 cells studied in each group.

D, I_{K+} *Left,* Voltage-gated potassium currents (I_{K+}) were evoked by 250 ms voltage steps from -80 to 90 mV following a 250 ms prepulse to -140 mV to remove inactivation. I_{K+} was studied during perfusion with control bath solution (upper, △) and then with the addition of 10 μM MG (lower, O). *Right,* Mean peak current-density ± SEM for 10 cells is plotted against test voltage for each condition.

E, I_{DR} *Left,* The delayed rectifier current, I_{DR}, was studied in the same cells that were used to study I_{K+} (panel D). I_{DR} was evoked by the protocol described in D, with the prepulse voltage changed to -50 mV to promote inactivation. The effect of 10 μM MG (O) was tested for each cell and the currents plotted (*right*) as mean peak current-density ± SEM against test voltage.

F, I_{KA} The inactivating component of current (I_{KA}) was calculated by subtracting I_{DR} (panel E) from I_{K+} (panel D). I_{KA} is shown as both current families (*left*) and as mean current density plots (*right*).

G, I_{GLY} MG did not modulate currents evoked by the application of 100 μM glycine to CGNs voltage clamped at -50 mV. Glycinergic currents, but not currents activated by 10 μM MG, were blocked by 500 nM strychnine. Bars represent the mean peak current-density ± SEM for 10 cells in each group.

H, I_{Glu} MG did not modulate currents evoked by application of 10 μM glutamate to CGNs that were voltage clamped at -50 mV in the absence of 1 mM extracellular magnesium. Glutamatergic currents, but not currents activated by 10 μM MG, were blocked by co-application of the NMDA receptor antagonist, AP-5, and the AMPA and kainate receptor antagonist, CNQX. The magnitude of the MG activated current was not dependent on extracellular magnesium. Bars represent the mean peak current-density ± SEM for ten cells in each group.

Figure S8 (continued)

I, The magnitude of the MG activated current was not altered by the presence or absence of 1 mM extracellular calcium. Bars represent the mean peak current-density ± SEM for ten cells in each group.

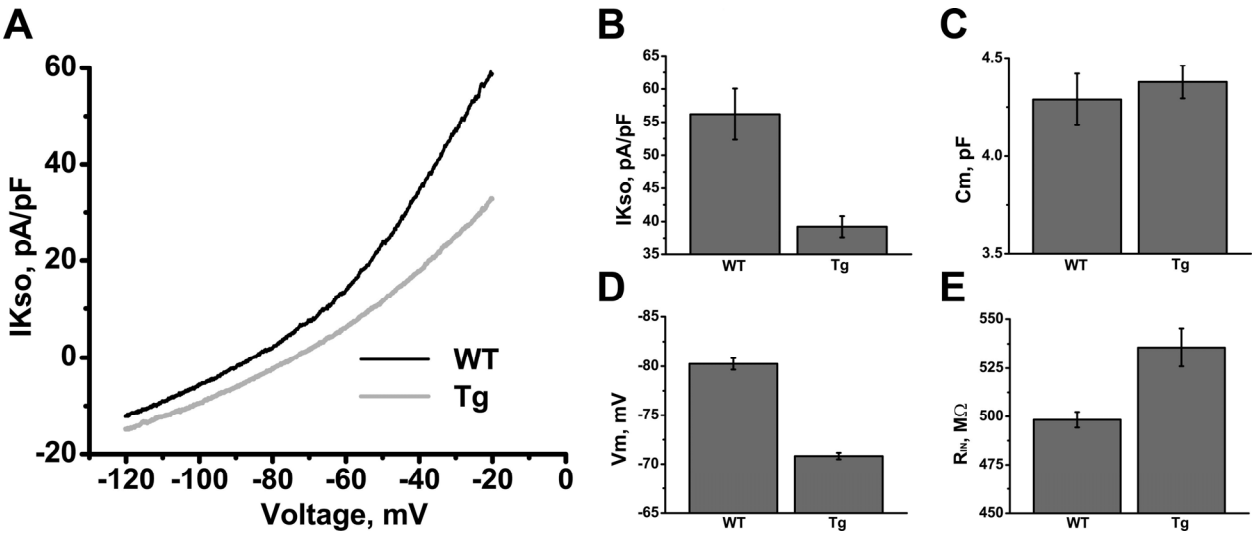

Figure S9: The excitability of CGN cultured from wild type and BAC littermate mice

CGN were cultured from WT and Tg littermates. *IKso*, membrane potential (Vm), and cellular input resistance (Rin) were determined.

A, Representative recordings demonstrate that *IKso* was smaller in Tg CGN compared to WT CGN, indicating increased excitability. **B,** A histogram of mean *IKso* from each group at -20 mV normalized to capacitance. **C,** Mean cell capacitance was not difference between WT and Tg CGN. **D,** Studying V_m revealed that Tg neurons were depolarized compared with WT neurons. **E,** Mean R_{in} was larger in Tg neurons, indicating increased excitability. All histograms represent mean ± SEM. n = 18 WT, 58 Tg.

The mechanism underlying these differences remains unknown. *IKso* is mediated primarily by K2P channels and, to a smaller extent, by tonic Cl^- conductance through $GABA_A$ receptors. Therefore, differences between WT and Tg neurons could represent changes in the in the composition or activity of K2P channel or $GABA_A$ receptor populations. While reduced activation of $GABA_A$ receptors is consistent with the reduced MG concentration observed in Tg

Figure S9 (continued)

mice (Figure 3C) and MG's activation of $GABA_A$ receptors (Figure 5 and Figure 6), the cells in this experiment were continuously perfused. Therefore, a difference in MG concentration could only mediate this effect if there were large concentrations or long-lasting effects at the synaptic cleft. However, application of diazepam, midazolam, and zolipem alone did not evoke currents in HN (data not shown), indicating negligible MG and GABA concentrations. Alternatively, this finding could reflect a long-term difference in ion channels at the cell membrane, such as K2P channels, or a difference in receptor function as the result of chronic differences in MG levels. Further studies will be important for investigating these possibilities.

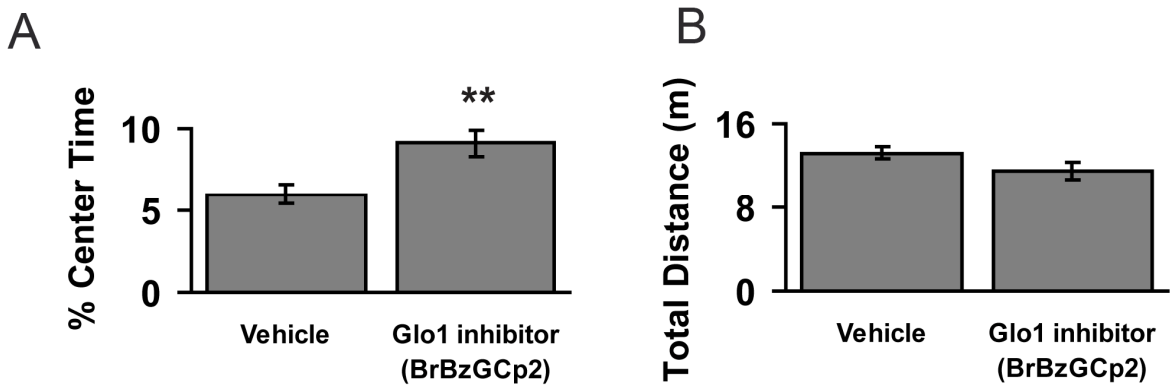

Figure S10: Glo1 inhibition decreases anxiety-like behavior in CD-1 mice

Male CD-1 mice were treated i.p. with vehicle or BrBzGCp2 (50 mg/kg). Two hours post-injection, mice were tested in the OF test. *n* = 19 vehicle, 19 BrBzGCp2. **A**, Mice treated with BrBzGCp2 spent more time in the center of the OF. **B**, BrBzGCp2 did not affect total distance traveled in the OF.

Data are mean ± SEM. BrBzGCp2, Bromobenzyl glutathione dicyclopentyl ester; OF, open field. $^{**}P < 0.005$.

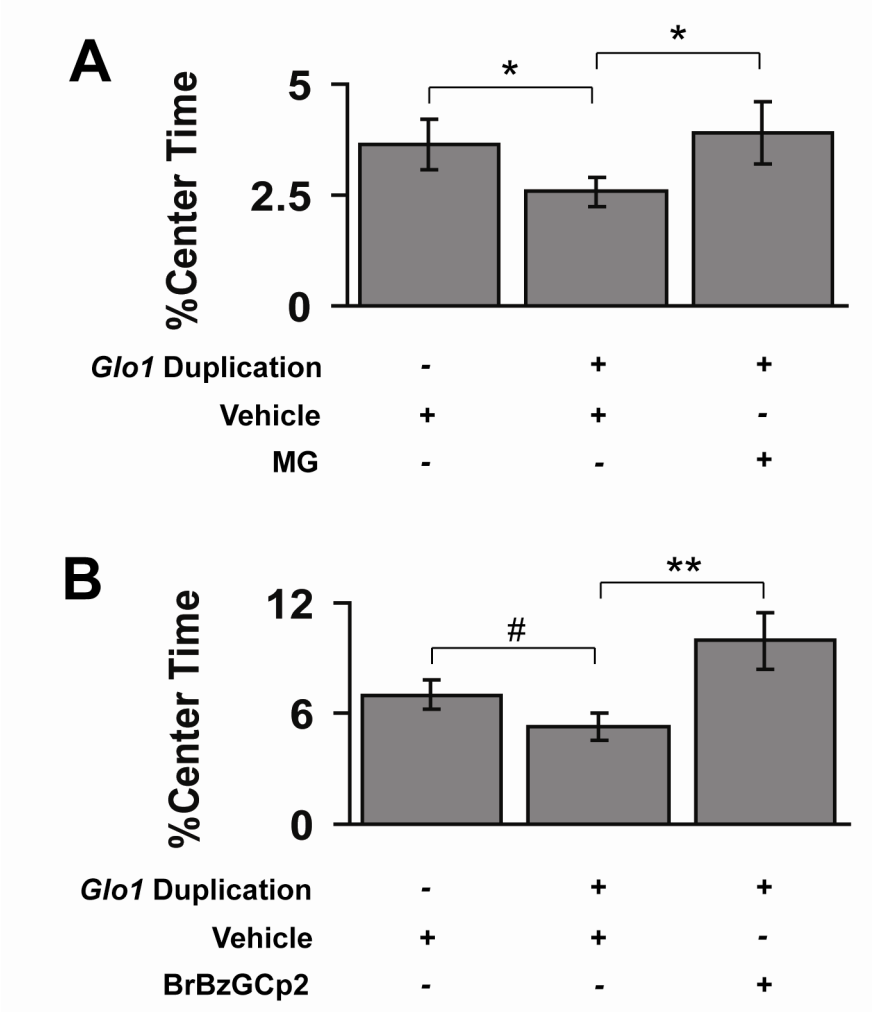

Figure S11: MG treatment and GLO1 inhibition rescue GLO1's anxiogenic effect

Male CD-1 mice were genotyped for the presence or absence of the *Glo1* duplication. **A,** Mice were treated i.p. with vehicle or MG (50 mg/kg). Ten minutes post-injection, mice were tested in the OF test. Mice with the *Glo1* duplication spent less time in the center of the OF. MG treatment reversed this effect. n = 12 non-duplicated treated with vehicle, 15 duplicated treated with vehicle, 15 duplicated treated with MG. **B,** Mice were treated i.p. with vehicle or BrBzGCp2 (50 mg/kg). Two hours post-injection, mice were tested in the OF test. Mice with the *Glo1* duplication spent less time in the center of the OF. GLO1 inhibition reversed this effect. n = 8

Figure S11 (continued)

non-duplicated treated with vehicle, 11 duplicated treated with vehicle, 9 duplicated treated with BrBzGCp2.

Data are mean ± SEM. BrBzGCp2, Bromobenzyl glutathione dicyclopentyl ester; OF, open field. #$P < 0.08$, *$P < 0.05$, **$P < 0.005$ by 1-tailed t-test.

Detailed Methods:

Animals: Behavioral tests used 7–10-week-old male mice. WT B6 mice were obtained from the Jackson Laboratory; CD-1 mice were obtained from Charles River; Tg mice were bred in-house. Tg mice were tested in parallel with their WT littermates. WT mice from each line did not significantly differ and were pooled. Primary cerebellar granule neurons were cultured from mixed-sex Sprague-Dawley rats. All procedures were approved by the University of Chicago's IACUC. Hippocampal neurons were a gift from Dr. Suzanne Paradis (Brandeis University, Waltham, MA).

BAC transgenic mice: The mouse BAC RP23-247F19 was obtained from CHORI and modified by RED/ET recombination (13). To prevent expression of alternatively spliced variants of *Btbd9* and *Dnahc8*, their first exons were replaced with ampicillin and kanamycin cassettes, respectively. The modified BAC was purified and injected into C57BL/6J or FVB/NJ pronuclei by the University of Chicago's Transgenic Core Facility. Positive founders that transmitted the BAC to their offspring were maintained as founder lines.

BAC copy number: Genomic DNA was used in qPCR with SYBR reagents (Applied biosystems). Primers targeted *Glo1* and a region of *Btbd9* outside the BAC. *Glo1* copy number was determined using the $\Delta\Delta C_T$ method (14). WT B6 and FVB mice have 2 copies of *Glo1* (15), so BAC copy number was calculated as (Fold change v. WT $\times$ 2) - 2.

General health and reflexes: Body position and righting, toe pinch, ear twitch, whisker orienting, and eye blink reflexes were scored as previously described (1). The whisker placing and visual placing responses were scored as previously described (16). The balance beam test was performed as previously described (17).

Microarray: Microarrays were Mouse Gene 1.0 ST Arrays (Affymetrix). Whole brains were dissected, snap frozen, and stored at -80°C until use. RNA was extracted using TRIzol (Invitrogen) and was cleaned using the RNeasy kit (Qiagen). RNA samples were transferred on dry ice to Precision Biomarker Resources, who processed the samples and performed all procedures, including data analysis. Statistical analyses were performed by converting *P*-values into q-values using Q-value software (18). Microarray data are available from GEO (http://www.ncbi.nlm.nih.gov/geo/) under accession number GSE36819.

qPCR for mRNA expression: RNA was extracted using the RNeasy kit with DNase digestion (Qiagen). cDNA was generated by reverse transcription (MultiScribe, Applied Biosystems) using oligo dT primers (Invitrogen). cDNA was used as a template in qPCR using SYBR reagents (Applied Biosystems). Primers targeted *Glo1* and β-*actin*. *Glo1* was normalized to *β-actin* and reported as fold change versus WT using the $2^{-\Delta\Delta CT}$ method (14).

Immunoblot: Tissue was homogenized in RIPA buffer. Twenty μg of protein was separated by SDS-PAGE and transferred to a PVDF membrane. Membranes were probed with primary antibodies against GLO1 (1:15,000, gift from Dr. Iiris Hovatta, University of Helsinki, Helsinki, Finland) and GAPDH (1:5,000, Cell Signaling Technology). Peroxidase-conjugated secondary antibodies were used (1:100,000, Jackson ImmunoResearch). Blots were developed with ECL plus (Thermo Scientific), digitized, and band intensity was measured by densitometry using NIH ImageJ software. Glo1 band intensity was normalized to GAPDH.

Open field test: The OF test was administered as previously described (15). The center size was 18 × 18 cm. Mice were placed into the center of the OF, and activity was monitored for 5 minutes. Data were collected and processed using the manufacturer's software (AccuScan Instruments). For studies with Tg mice, WT and Tg littermates and were tested in parallel. WT

mice did not significantly differ between lines and were pooled into a common control group. Mice that differed by more than 2 standard deviations from the mean were excluded. When we performed statistical analyses including the outliers, the results remained statistically significant.

Light-dark box test: Mice were placed in the light compartment, and activity was monitored for 4 minutes. Behavior was recorded and automatically scored by the Noldus Ethovision System.

Elevated plus maze: The elevated plus maze (Stoelting) consisted of four arms measuring 5 cm × 35 cm; the two closed arms had 15-cm high walls. The apparatus was raised 40 cm above the ground, and was illuminated to 15 lux. The animal was placed into the center of the apparatus, and behavior was scored for 5 minutes.

Enzymatic activity: Glo1 activity was assayed by measuring the rate of formation of S-D-lactoylglutathione (19). Tissue was homogenized in 0.1 M sodium phosphate buffer, pH 7.5, 1 mM EDTA, and proteinase inhibitors. Brain homogenate (10–50 μg protein) was added to a hemithioacetal substrate (2 mM MG and 2mM GSH, both obtained from Sigma-Aldrich) and absorbance at 240 nm was measured every 30 seconds for 4 minutes.

HPLC: MG concentration was measured by HPLC as previously described (7) with modifications. Tissue was homogenized in 50 mM sodium phosphate buffer, pH 6.6 and 0.8N perchloric acid, incubated on ice for 10 minutes, and centrifuged. The supernatant was filtered, and MG was derivatized with 10 mM *o*-phenylenediamine to form 2-methylquinoxaline (2-MQ). Fifteen μM 5-methylquinoxaline (5-MQ) was spiked into each sample as an internal standard. 2-MQ was quantified using an HP 1100 HPLC system (Agilent) with a Nova-Pak C18 column (Waters Corporation). Column effluent was monitored at 315 nm. 2-MQ concentration was determined by comparison to 2-MQ standards of known mass. Quantification of 2-MQ was

corrected for losses by comparison with 5-MQ. MG concentration was calculated as 2-MQ/tissue weight.

Methylglyoxal pharmacology in vivo:

Treatment: MG was obtained from Sigma-Aldrich, filter-sterilized (0.22 μm filter, Millipore), diluted in vehicle (0.9% NaCl), and adjusted to pH ~ 7.4. Mice were injected i.p. with 10 ml/kg MG or vehicle.

HPLC: Ten minutes post-injection, mice were sacrificed, and the brain was rapidly dissected and flash-frozen on dry ice. MG concentration was measured as described above.

Open field test: Ten minutes post-injection, mice were placed into the center of the OF. Behavior was measured as described above.

Open field test replication studies: Ten to twenty minutes post-injection, mice were tested in the OF for 5–10 minutes. In some experiments, behavior was scored as described above. In other experiments, mice were tested in the OF, and behavior was automatically scored by the Noldus Ethovision System.

Meta-analysis: Results from individual experiments were compiled and analyzed with MIX 1.7 software using a fixed-effect model (20).

Light-dark box test: Ten minutes post-injection, mice were placed in the light compartment, and activity was monitored for 3 minutes. Behavior was recorded and automatically scored by the Noldus Ethovision System.

Balance beam: The balance beam test was performed as previously described (17). The balance beam was 97 cm × 9.5 mm and elevated to 46 cm. 10 minutes post-injection, mice were tested on the balance beam, and missteps were recorded. Data were analyzed using non-parametric statistics, because vehicle-treated mice generally did not make errors.

Hypothermia: 30 minutes post-injection, rectal temperature was measured by digital thermometer.

TUNEL staining: WT B6 male mice were treated i.p. with vehicle or MG (50 or 300 mg/kg). Twenty-four hours post-injection, mice were anesthetized with ketamine (100 mg/kg) and xylazine (10 mg/kg). Mice were transcardially perfused with PBS, pH 7.4. Brains were dissected and post-fixed for 48 hours in 4% paraformaldehyde, pH 7.4. Fixed brains were washed in PBS and placed in 70% ethanol until processing. Brains were submitted to the University of Chicago's Human Tissue Resource Center for processing. Brains were embedded in paraffin, sectioned to 5 μm, TUNEL stained using the ApopTag Plus Peroxidase In Situ Apoptosis Detection Kit (Millipore) according to the manufacturer's instructions, and counterstained with hematoxylin. Slides were digitally scanned with ScanScope XT (Aperio Technologies). Images were analyzed using Spectrum Plus software (Aperio Technologies) to count TUNEL-positive cells and total cells in each section. %TUNEL positive values were calculated as: (TUNEL positive cells/Total cells) × 100%. A positive control (female rodent mammary gland 3–5 days post-weaning, provided in the kit) was stained and analyzed in parallel with the experimental samples.

Electrophysiology:

*Reagent*s: All reagents were obtained from Sigma-Aldrich. Pure MG was also synthesized in-house; electrophysiological results were identical between pure MG and MG obtained from Sigma-Aldrich. MG, GABA, glycine, L-glutamate, SR-95531, strychnine, CNQX, AP-5, diazepam, midazolam, and zolpidem were applied with a computer controlled MPS-2 multichannel perfusion system (WPI).

Culture of rat cerebellar granule neurons: Tissue was dissected from 6- to 8-day-old rats. Cells were suspended in minimum essential medium supplemented with 10% fetal calf serum, 26 mM glucose, 19 mM KCl, 2 mM L-glutamine, and penicillin/streptomycin (50 IU/ml and 50 μg/ml). Cells were seeded on poly-L-lysine-coated coverslips and incubated in a humidified atmosphere containing 5% CO_2 at 37°C. After 48 hours, the culture medium was replaced with minimum essential medium supplemented with 10% horse serum, 26 mM glucose, 19 mM KCl, 2 mM L-glutamine, penicillin/streptomycin (50 IU/ml and 50 μg/ml), and 80 μM L-fluorodeoxyuridine. Culture medium was exchanged every 3 days. All recordings were made from cells between days 6 to 9 in culture.

Culture of rat hippocampal neurons: Hippocampal neurons were prepared from E17 Sprague-Dawley rats as previously described (21) and seeded to poly-L-lysine coated glass coverslips. Neurons were maintained in Neurobasal medium with B27 supplement and Glutamax, in a humidified atmosphere with 5% CO_2 at 37ºC.

Whole-cell patch clamp: Whole-cell patch-clamp was performed as previously described (22) using an Axopatch 200B amplifier and pCLAMP software (Molecular Devices) at filter and sampling frequencies of 5 and 25 kHz, respectively, for voltage-clamp experiments and 1 and 10 kHz, respectively, for current-clamp recording. Experiments were performed at 32°C using a feedback-controlled heated perfusion system (Warner Instruments). V_m, ligand-gated, and potassium channel currents were studied in a bath solution containing 1 mM $CaCl_2$, 1 mM $MgCl_2$, 4 mM KCl, 140 mM NaCl, 5 mM glucose, and 10 mM HEPES, pH 7.4. Electrodes were fabricated from borosilicate glass (Clark) and had a resistance of 4–5 MΩ when filled with a solution containing 136 mM KCl, 1 mM $MgCl_2$, 2 mM K_2ATP, 5 mM EGTA, and 10 mM HEPES, pH 7.2. Electrodes were coated with Sigmacote (Sigma) prior to use.

Macropatch recording: Macropatch recording was performed with 1.5–2 MΩ electrodes filled with bath solution. The inside of excised patches was perfused with electrode solution containing the indicated reagents. SR-95531 was added to the electrode where indicated.

Potassium currents: Voltage-gated potassium channel currents were evoked using a previously reported protocol with modifications (22). The whole voltage-gated potassium current, I_{K+}, and the delayed rectifier current, I_{DR} were isolated with two voltage-protocols. First, I_{K+} was evoked by 250 ms test pulses to between -80 and 90 mV from -80 mV following a 250 ms pre-pulse to -140 mV. Then, the protocol was repeated using a -50 mV pre-pulse to inactivate I_{K+} and isolate I_{DR}. The inactivating component of current, I_{KA}, was isolated by subtracting I_{DR} from I_{K+} recorded in the same cells. The standing outward potassium leak current, *IKso*, and the inwardly rectifying potassium current, I_{KIR}, were studied as previously reported with modifications (23). Cells were held at -20 mV, and the membrane potential was ramped to -120 mV over a period of 100 ms before returning to -20 mV. Ramp hyperpolarizations were repeated every 20 seconds.

Sodium currents: Sodium currents were studied as previously described (24) using a bath solution containing 130 mM NaCl, 5 mM CsCl, 2 mM $CaCl_2$, 1.2 mM $MgCl_2$, 5 mM glucose, and 10 mM HEPES adjusted to pH 7.4 with NaOH. Tetrodotoxin (Sigma) at a final concentration of 500 nM was included in the bath to block voltage-gated sodium currents. The electrode solution contained 60 mM CsCl, 80 mM CsF, 10 mM EGTA, 1 mM $CaCl_2$, 1 mM $MgCl_2$, 5 mM Na_2ATP, and 10 mM HEPES adjusted to pH 7.4 with CsOH. All voltage-gated currents were studied following a P/5 leak subtraction protocol, and voltage-clamp errors were minimized with 80% series resistance compensation.

Ligand-gated currents: Ligand-gated currents were studied in voltage-clamp mode by application of reagents to cells held at -50 mV. GABAergic and glycinergic currents were

activated by application of GABA and glycine and antagonized by application of SR-95531 and strychnine, respectively (25). Glutamatergic currents were activated by L-glutamate and antagonized by CNQX and AP-5 (26).

Glo1 inhibitor:

BrBzGCp2 synthesis: BrBzGCp2 was prepared on a multigram scale in two steps from reduced glutathione as previously described with modifications (27, 28). Reduced glutathione was reacted with 4-bromobenzylbromide and sodium hydroxide in ethanol for 10 days followed by acidification with HI to pH 3.5 and filtration to give bromobenzylglutathione (28) as a bright white solid (27). This was then esterified with excess acidified cyclopentanol to give crude BrBzGCp (28) as a mixture of mono- and diesters. The desired diester is moderately soluble in diethyl ether, whereas the monoester is virtually insoluble. Repeated suspension of the crude product in diethyl ether, followed by filtration and evaporation of the filtrate, gave the desired BrBzGCp2 in >95% purity as assessed by NMR.

Enzymatic activity: Vehicle (DMSO) or 100 μM BrBzGCp2 was added to 10 ng of purified human Glo1. Enzymatic activity was measured as described above.

Treatment: BrBzGCp2 was dissolved in vehicle (8% DMSO and 18% Tween-80). Mice were treated i.p. with 10 ml/kg BrBzGCp2 or vehicle.

HPLC: Two hours post-injection, mice were sacrificed, and brains were rapidly dissected and flash-frozen on dry ice. MG concentration was measured as described above.

OF test: Two hours post-injection, mice were tested in the OF test as described above. The center size was 10×10 cm.

***Glo1* duplication genotyping:** CD-1 mice were genotyped for the presence or absence of the *Glo1* duplication using PCR as previously reported (15).

Supplementary References

1. Crawley, J.N. 2007. *What's Wrong with My Mouse?*: Wiley-Liss.
2. Bouwknecht, J.A., and Paylor, R. 2008. Pitfalls in the interpretation of genetic and pharmacological effects on anxiety-like behaviour in rodents. *Behav Pharmacol* 19:385-402.
3. Kurz, A., Rabbani, N., Walter, M., Bonin, M., Thornalley, P., Auburger, G., and Gispert, S. 2011. Alpha-synuclein deficiency leads to increased glyoxalase I expression and glycation stress. *Cellular and Molecular Life Sciences* 68:721-733.
4. Hambsch, B., Chen, B.G., Brenndorfer, J., Meyer, M., Avrabos, C., Maccarrone, G., Liu, R.H., Eder, M., Turck, C.W., and Landgraf, R. 2010. Methylglyoxal-mediated anxiolysis involves increased protein modification and elevated expression of glyoxalase 1 in the brain. *J Neurochem* 113:1240-1251.
5. Jia, X., and Wu, L. 2007. Accumulation of endogenous methylglyoxal impaired insulin signaling in adipose tissue of fructose-fed rats. *Mol Cell Biochem* 306:133–139.
6. Wang, X., Jia, X., Chang, T., Desai, K., and Wu, L. 2008. Attenuation of hypertension development by scavenging methylglyoxal in fructose-treated rats. *Journal of Hypertension* 26:765–772.
7. Dhar, A., Desai, K., Liu, J., and Wu, L. 2009. Methylglyoxal, protein binding and biological samples: are we getting the true measure? *J Chromatogr B Analyt Technol Biomed Life Sci* 877:1093-1100.
8. Randella, E.W., Vasdevb, S., and Gill, V. 2005. Measurement of methylglyoxal in rat tissues by electrospray ionization mass spectrometry and liquid chromatography. *Journal of Pharmacological and Toxicological Methods* 51:153–157.
9. Lu, J., Randell, E., Han, Y., Adeli, K., Krahn, J., and Meng, Q. 2011. Increased plasma methylglyoxal level, inflammation, and vascular endothelial dysfunction in diabetic nephropathy. *Clin Biochem* 44:307-311.
10. Cohen, J. 1988. *Statistical Power Analysis for the Behavioral Sciences*. Hillsdale: Lawrence Erlbaum Associates, Inc.
11. Stoltenburg-Didinger, G. 1994. Neuropathology of the hippocampus and its susceptibility to neurotoxic insult. *Neurotoxicology* 15:445-450.
12. Di Loreto, S., Zimmitti, V., Sebastiani, P., Cervelli, C., Falone, S., and Amicarelli, F. 2008. Methylglyoxal causes strong weakening of detoxifying capacity and apoptotic cell death in rat hippocampal neurons. *Int J Biochem Cell Biol* 40:245-257.
13. Copeland, N.G., Jenkins, N.A., and Court, D.L. 2001. Recombineering: a powerful new tool for mouse functional genomics. *Nat Rev Genet* 2:769-779.
14. Schmittgen, T.D., and Livak, K.J. 2008. Analyzing real-time PCR data by the comparative C(T) method. *Nat Protoc* 3:1101-1108.
15. Williams, R.t., Lim, J.E., Harr, B., Wing, C., Walters, R., Distler, M.G., Teschke, M., Wu, C., Wiltshire, T., Su, A.I., et al. 2009. A common and unstable copy number variant is associated with differences in Glo1 expression and anxiety-like behavior. *PLoS One* 4:e4649.
16. Fox, W.M. 1965. Reflex-ontogeny and behavioural development of the mouse. *Anim Behav* 13:234-241.

17. Crabbe, J.C., Metten, P., Yu, C.H., Schlumbohm, J.P., Cameron, A.J., and Wahlsten, D. 2003. Genotypic differences in ethanol sensitivity in two tests of motor incoordination. *J Appl Physiol* 95:1338-1351.
18. Storey, J.D., and Tibshirani, R. 2003. Statistical significance for genomewide studies. *Proc Natl Acad Sci U S A* 100:9440-9445.
19. Allen, R.E., Lo, T.W., and Thornalley, P.J. 1993. A simplified method for the purification of human red blood cell glyoxalase. I. Characteristics, immunoblotting, and inhibitor studies. *J Protein Chem* 12:111-119.
20. Bax, L., Yu, L., Ikeda, N., Tsuruta, N., and Moons, K. 2006. Development and validation of MIX: Comprehensive free software for meta-analysis of causal research data. *BMC Medical Research Methodology* 6.
21. Plant, L.D., Dowdell, E.J., Dementieva, I.S., Marks, J.D., and Goldstein, S.A. 2011. SUMO modification of cell surface Kv2.1 potassium channels regulates the activity of rat hippocampal neurons. *J Gen Physiol* 137:441-454.
22. Plant, L.D., Webster, N.J., Boyle, J.P., Ramsden, M., Freir, D.B., Peers, C., and Pearson, H.A. 2006. Amyloid beta peptide as a physiological modulator of neuronal 'A'-type K+ current. *Neurobiol Aging* 27:1673-1683.
23. Plant, L.D., Kemp, P.J., Peers, C., Henderson, Z., and Pearson, H.A. 2002. Hypoxic depolarization of cerebellar granule neurons by specific inhibition of TASK-1. *Stroke* 33:2324-2328.
24. Plant, L.D., Bowers, P.N., Liu, Q., Morgan, T., Zhang, T., State, M.W., Chen, W., Kittles, R.A., and Goldstein, S.A. 2006. A common cardiac sodium channel variant associated with sudden infant death in African Americans, SCN5A S1103Y. *J Clin Invest* 116:430-435.
25. Kaneda, M., Farrant, M., and Cull-Candy, S.G. 1995. Whole-cell and single-channel currents activated by GABA and glycine in granule cells of the rat cerebellum. *J Physiol* 485 (Pt 2):419-435.
26. Wyllie, D.J., and Cull-Candy, S.G. 1994. A comparison of non-NMDA receptor channels in type-2 astrocytes and granule cells from rat cerebellum. *J Physiol* 475:95-114.
27. Vince, R., Daluge, S., and Wadd, W.B. 1971. Studies on the inhibition of glyoxalase I by S-substituted glutathiones. *J Med Chem* 14:402-404.
28. Thornalley, P.J., Ladan, M.J., Ridgway, S.J., and Kang, Y. 1996. Antitumor activity of S-(p-bromobenzyl)glutathione diesters in vitro: a structure-activity study. *J Med Chem* 39:3409-3411.